Encoding of configural regularity in the human visual system

Jonas Kubilius Laboratories of Biological and Experimental Psychology, KU Leuven, Leuven, Belgium

Johan Wagemans Laboratory of Experimental Psychology, KU Leuven, Leuven, Belgium

Hans P. Op de Beeck Laboratory of Biological Psychology, KU Leuven, Leuven, Belgium

The visual system is very efficient in encoding stimulus properties by utilizing available regularities in the inputs. To explore the underlying encoding strategies during visual information processing, we presented participants with two-line configurations that varied in the amount of configural regularity (or degrees of freedom in the relative positioning of the two lines) in a fMRI experiment. Configural regularity ranged from a generic configuration to stimuli resembling an "L" (i.e., a right-angle L-junction), a "T" (i.e., a right-angle midpoint T-junction), or a "+",—the latter being the most regular stimulus. We found that the response strength in the shape-selective lateral occipital area was consistently lower for a higher degree of regularity in the stimuli. In the second experiment, using multivoxel pattern analysis, we further show that regularity is encoded in terms of the fMRI signal strength but not in the distributed pattern of responses. Finally, we found that the results of these experiments could not be accounted for by low-level stimulus properties and are distinct from norm-based encoding. Our results suggest that regularity plays an important role in stimulus encoding in the ventral visual processing stream.

Introduction

The brain is subject to processing huge amounts of information, and thus, efficiency in information encoding is often postulated as one of the major organizing principles in the brain (Attneave, 1954, 1959; Barlow, 1961; Simoncelli & Olshausen, 2001; Friston, 2009). In the visual system, efficiency has been observed at many levels, including highly optimized information transmission and redundancy in the retinal ganglion cells (Doi et al., 2012), sparse encoding strategy of natural images in V1 (Vinje & Gallant, 2000), and utilization of higher-order stimulus regularities in midlevel and high-level vision (Kourtzi & Connor, 2011).

It is natural to expect that efficient representations would be maximally informative with respect to the actual inputs in the world. In particular, stimuli that are more likely to occur should be encoded more compactly. The primate visual system has long been known to utilize such perceptual regularities (DiCarlo & Cox, 2007; Wagemans, Elder et al., 2012; Wagemans, Feldman et al., 2012). For example, in natural scenes, elements tend to be cocircular, and the visual system appears to be sensitive to such regularity (Geisler, Perry, Super, & Gallogly, 2001; Sigman, Cecchi, Gilbert, & Magnasco, 2001). Another higher-level strategy, known as norm-based encoding (Leopold, O'Toole, Vetter, & Blanz, 2001; Op de Beeck, Wagemans, & Vogels, 2003; Rhodes & Jeffery, 2006), utilizes one particular regularity of the distribution of encountered exemplars from a given category, namely the center of this distribution. For example, Leopold and colleagues (2001) demonstrated that adaptation to faces results in a perceptual shift toward the center ("norm") in the face space and that single face-selective neurons in the macaque monkey are tuned to the average (Leopold, Bondar, & Giese, 2006), arguing that such strategy minimizes resources the system needs to learn and store stimuli.

In addition to the frequency of co-occurrence and centrality in a category, "coincidence avoidance" has been proposed as a general principle of visual processing as well. In general, the visual system prefers interpretations that are least likely to have resulted by accident (Rock, 1983; Biederman, 1987). More formally, Feldman (1997, 2009) argued that the visual system prefers the most regular (or most restricted) interpretation consistent with the input, and he

Citation: Kubilius, J., Wagemans, J., & Op de Beeck, H. P. (2014). Encoding of configural regularity in the human visual system. *Journal of Vision*, *14*(9):11, 1–17, http://www.journalofvision.org/content/14/9/11, doi:10.1167/14.9.11.

doi: 10.1167/14.9.11 Received September 2, 2013; published August 13, 2014 ISSN 1534-7362

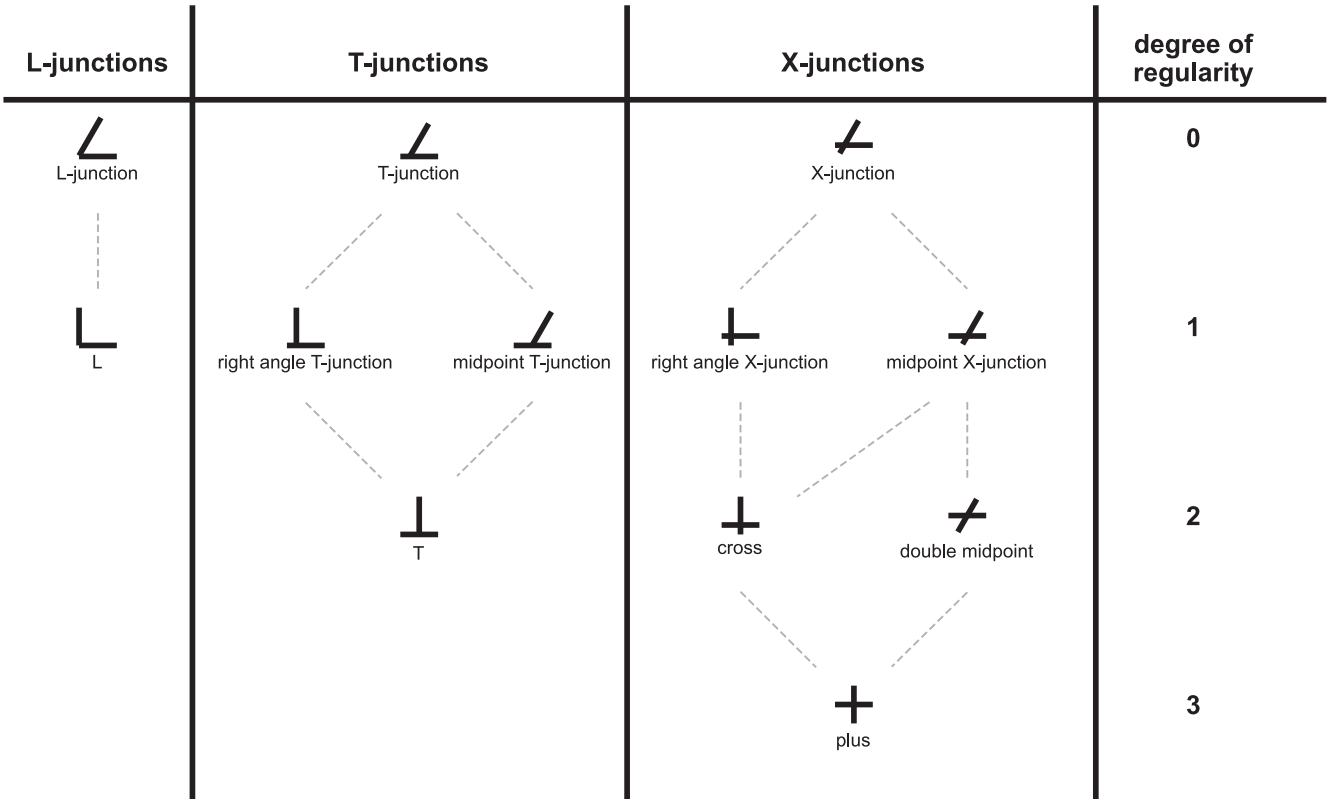

Figure 1. Two-line stimuli used in Experiment 1. Each stimulus belongs to one of the three junction classes, and within the class, stimuli are ordered by the degree of their regularity (Feldman, 2003, 2007). The most generic configurations are assigned a degree of regularity equal to zero (i.e., least regular). By constraining one degree of freedom at a time (in this case, angle or intersection position), the degree of regularity is increased by one. According to this scheme, a plus is the most regular two-line configuration (regularity is 3 in this hierarchy) with no degrees of freedom. (See Appendix for a comparison of this regularity definition to the strict version of Minimal Model Theory and SIT.)

proposed a partial ordering of stimuli in terms of their regularity. Consider, for example, the two-line configurations in Figure 1. At the top of the figure, configurations appear rather generic without any particular features that stand out. However, upon constraining one degree of freedom at a time (angle or position of intersection), these configurations gradually become more special in the sense that they contain more regularity and are more readily perceived as a distinct configuration (Feldman, 1992, 1997). For example, the upside-down T in Figure 1 is perceived to be a T in the 3-D world and not a skewed T (called "midpoint T-junction" in Figure 1) even though under certain conditions a skewed T could also project to an upside-down T. Given that such configurations can be encoded using shorter (simpler) descriptions with fewer parameters (van Lier, van der Helm, & Leeuwenberg, 1994; Leeuwenberg & van der Helm, 2012; van der Helm, 2014; see Appendix) or simpler generative models (Feldman, 2009), taking an advantage of such stimulus regularities might be both an optimal (maximally likely to be correct) and efficient processing strategy.

These largely theoretical proposals are potentially very important to understand how the visual system encodes regularity and have received some support from behavioral studies. For example, Feldman (2007) tested response times of detecting whether two dots presented either on a particular two-line configuration (same object condition) or on a separate line (different object condition). He hypothesized that more regular configurations would be bound more strongly (or would be better Gestalts), resulting in a higher benefit for within-object than between-objects task dot comparison. Feldman (2007) reported that, on average, reporting dots on the same object was easier for more regular configurations (see his Figure 9).

Using a different approach to regularity, van Lier and colleagues (1994) investigated various overlapping shapes that had several possible interpretations of the occluded part of a shape. For example, two overlapping rectangles could be interpreted as two rectangles (the preferred interpretation) or as a rectangle and another rectangle that has a corner missing (non-preferred interpretation). They computed the complexity (or structural information) of each

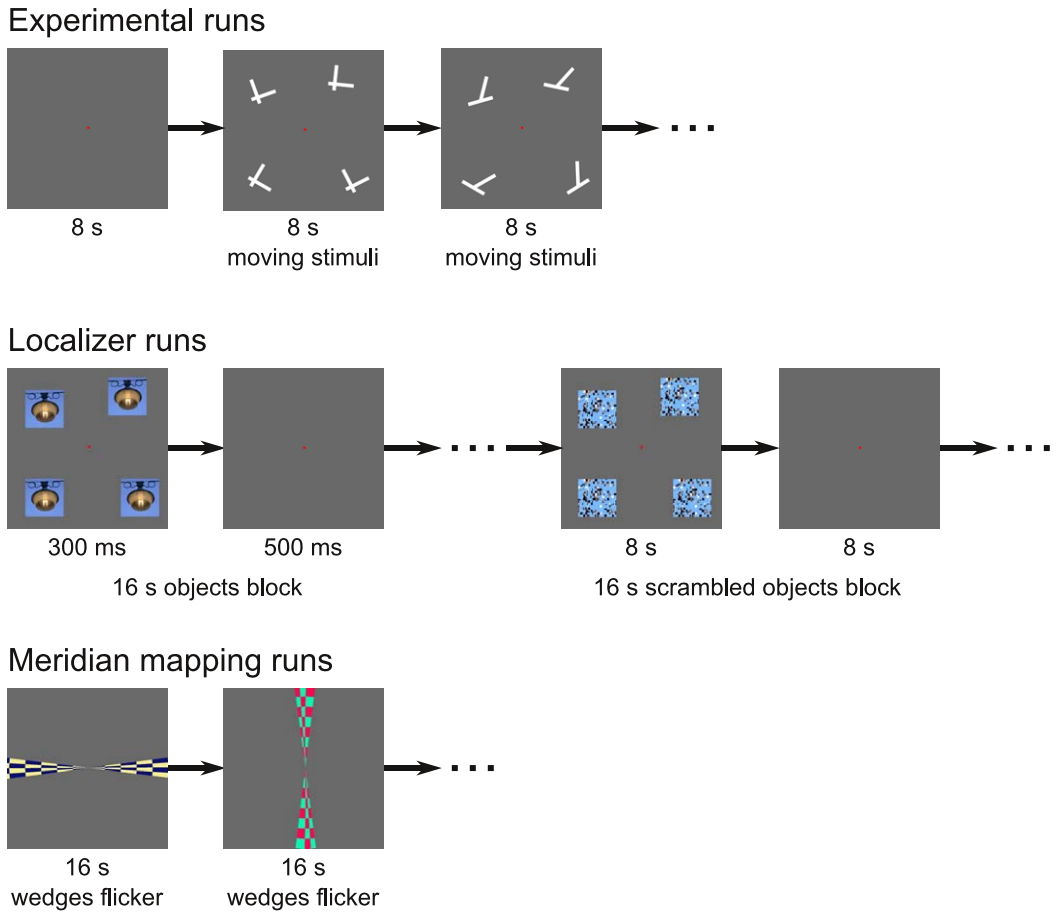

Figure 2. Illustration of trial sequences for the three types of runs used in the study. In experimental runs (top row), a display containing four identical two-line configurations was presented. A small amount of random position and orientation jitter was added to each stimulus separately at each frame, resulting in independent random smooth motion trajectories throughout the 8-s block. In the localizer runs (middle row), each trial consisted of a 300-ms presentation of four images (one of which did not match the others), followed by a 500-ms interstimulus interval. In the objects block, the images were intact, and in the scrambled-objects block, the images were scrambled. In meridian-mapping runs (bottom row), flickering wedges composed of checkerboard patterns were presented along either the horizontal or the vertical meridian. Wedges in each orientation were displayed for 16 s each.

interpretation and showed that the interpretation with a lower complexity score tended to agree with the preferred interpretation (as determined by observers) (see their figure 19).

However, very little is known about the neural encoding of this type of regularity. Hence, in this study, we wished to investigate whether the human visual system is sensitive to the available configural regularities in stimulus composition, defined as genericity or nonaccidentalness. We constructed a precisely controlled stimulus set in which each stimulus was composed of two lines but varied in the amount of intrinsic regularity. In two fMRI experiments, we demonstrate a reliable decrease of fMRI signal strength with an increase in stimulus regularity in the lateral occipital cortex (LO). Using model simulations of the primary visual cortex responses, we further show that responses in early visual areas to these stimuli are well described by their physical properties and similarity, but this effect is vanished in higher visual areas, implying that the observed dependency on stimulus regularity is (a) not a trivial consequence of low-level image processing, and (b) is distinct from norm-based encoding.

Experiment 1

Methods

All experiments, analyses, and simulations were coded in Python 2.7 using PsychoPy (Peirce, 2007, 2009), psychopy_ext (Kubilius, 2014), pandas, and PyMVPA2 (Hanke et al., 2009) packages (and their dependencies). Source code is available online at https://bitbucket.org/qbilius/twolines.

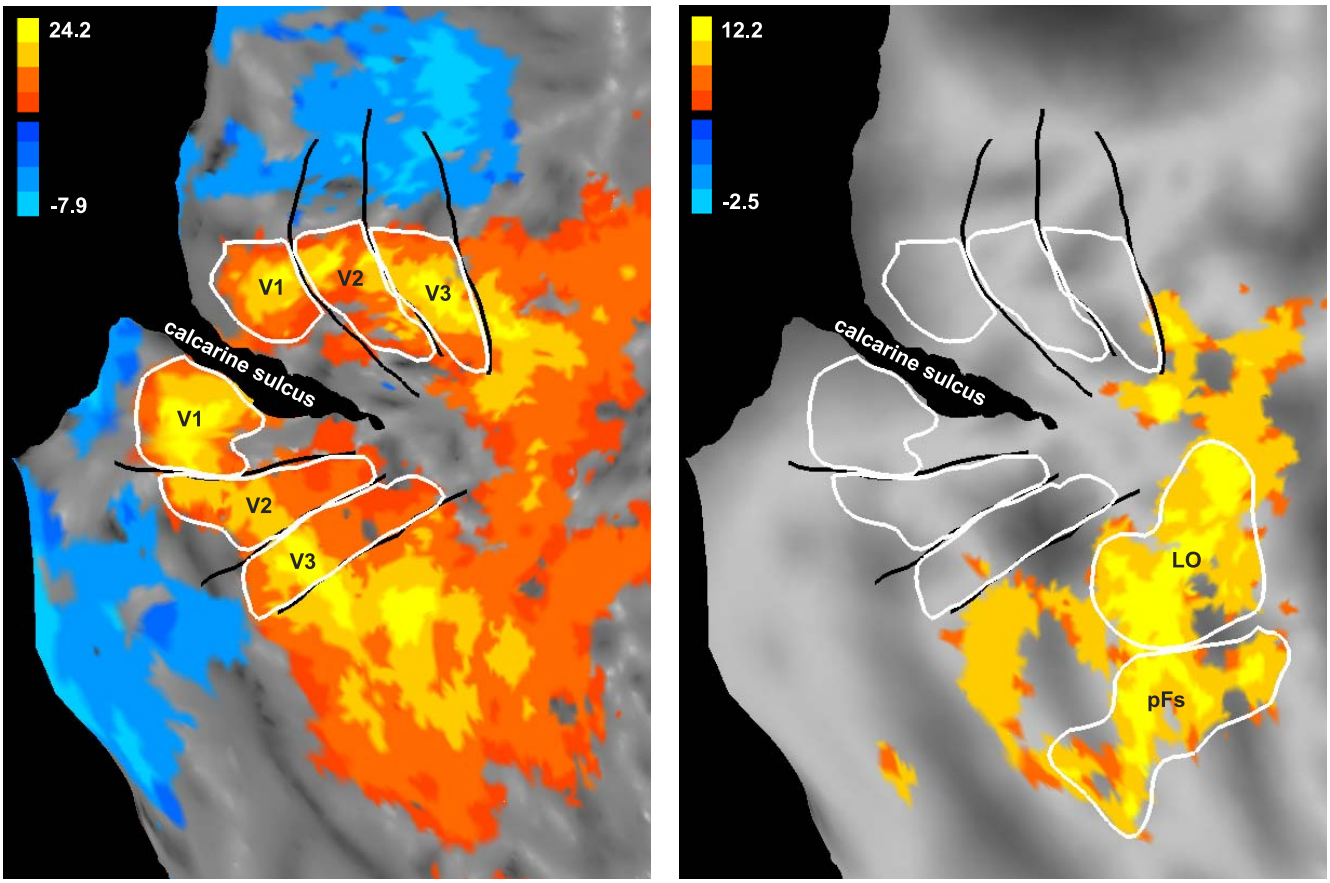

Figure 3. Flattened image of the right hemisphere for one participant with the borders of ROIs (white outlines). Black lines indicate borders between V1 and V2, V2 and V3, and V3 and higher regions, as identified using meridian-mapping. White regions mark the identified ROIs using the contrast all stimuli > fixation (V1, V2, V3; left panel; shown at $t = 3.765$ threshold) and objects > scrambled (LO, pFs, right panel; shown at $t = 5.70$ threshold) in the localizer task.

Participants

Ten affiliates of KU Leuven (ages 20–29, five males, five females) participated in the experiment. Two participants were excluded from further analyses after a failure to reconstruct the surface of their brain in Caret, resulting in eight participants whose data are reported here. The experiment was approved by the committee for medical ethics at KU Leuven.

Stimuli

We used two equal line segments to generate the stimulus space (Figure 1). With two segments touching or intersecting, only three classes of stimuli are possible: L-, T-, and X-junctions. Within each junction, we manipulated stimulus regularity by constraining the angle (either 90° or not) and the intersection of the two lines (either midpoint or not). Note that these two dimensions were not arbitrary; in fact, manipulating them is the only way to get from the most generic two-line configurations to the "L," "T," or "plus" stimuli. This procedure resulted in two stimuli with L-junctions, four stimuli with T-junctions, and six stimuli with X-junctions (12 stimulus conditions in total). Participants observed each stimulus separately and equally often in a blocked fMRI experiment (see "Experimental runs").

Junction index

We further confirmed that participants parsed stimulus space into three junction categories by computing a "junction index," which amounts to an average stimulus dissimilarity across junctions minus an average dissimilarity within the junction. If this junction index is significantly positive, it means that stimuli from a single junction type are more similar than across junctions, indicating that participants perceived each stimulus as belonging to a particular junction category. As expected, this computation yielded to a higher similarity within a junction type, most robustly in behavioral ratings, two-tailed one-sample t test: $t(7) = 12.8$, $p < 0.001$, and LO, $t(7) = 6.73$,

$p < 0.001$, but present in all regions of interest (ROIs) except posterior fusiform (pFs) ($ts > 2.64$, $ps < 0.033$).

fMRI scans

The fMRI experiment consisted of two scan sessions, 2 hr and 1.5 hr long, during which participants completed between 16 and 23 runs of the main task (248 s each), two localizer runs (336 s each), and two meridian-mapping runs (if not done before in other experiments with the same subjects; 336 s each). If not available from previous experiments, a high-resolution anatomical scan was conducted after all runs were completed.

Functional and anatomical MRI (fMRI) data were obtained using a 3-T Philips Achieva scanner with a 32-channel SENSE head coil using an echo-planar imaging sequence. For the functional runs, we recorded 36 slices oriented downward for the full inferotemporal cortex coverage (voxel size = 2.75 × 2.75 × 2.75 mm, interslice distance = 0.2 mm, acquisition matrix = 80 × 80). Each run consisted of 124 (experimental runs) or 168 (localizer and meridian-mapping runs) measurements; the interval between measurements (repetition time) was set to 2 s with an echo time of 30 ms. The T1-weighted anatomical scan had 0.85 × 0.98 mm in-plane resolution, 1.37 mm between the slices (acquisition matrix = 256 × 256), a 9.6-ms repetition time, a 4.6-ms echo time, 182 coronal slices, and a duration of 383 s.

Experimental runs

Participants observed displays of four identical stimuli (although with some position and orientation jitter) in the quadrants of the visual field (Figure 2). Stimuli were presented in blocks of 8 s, during which they were smoothly moving (within ±5° for the rotation and ±0.25° for the position). Participants were asked to judge the similarity of the current display to the previous display on a scale of 1 to 4. They responded using a two-button button box: 1 (very dissimilar) = button 1 twice, 2 (dissimilar) = button 1 once, 3 (similar) = button 2 once, 4 (very similar) = button 2 twice.

Stimuli were composed of two lines equal in length (2° length, 0.3° width), intersecting at either one fourth or one half of the line length at either a 60° or 90° angle. They were white and presented on a gray background 3° away from the central red fixation dot (0.2° size), which was used to maintain a stable fixation during the scans. All 12 stimuli in Figure 1 were presented equally often in a palindromic order (determined by a Latin square), resulting in each condition being presented twice per run. Stimuli were interleaved every four blocks by a fixation block in which only a fixation dot was present for 8 s. Also, each run started and ended with an 8-s fixation block. In total, each experimental run took 248 s.

Localizer runs

The localizer runs were designed to localize both shape-selective and retinotopic brain areas that were activated by the four stimuli locations in the experimental runs. We modified a standard localizer containing intact and scrambled objects (Grill-Spector et al., 1998) to present four identical images in the four quadrants (images taken from morgueFile.com as permitted by the morgueFile free license and ImageAfter.com as permitted by the ImageAfter license). Stimuli were presented in blocks of 20 (i.e., there were 20 different images and 20 different scrambled images in total) for 300 ms (followed by a 500-ms fixation display) approximately 3° away from a central fixation dot (with an offset matching that of the stimuli) and subtended 3° of visual angle (to ensure we captured the whole region occupied by the stimuli in the experimental runs). Participants were asked to press a key when images were shown greatly reduced in contrast.

Meridian-mapping runs

We used a standard procedure for the meridian-mapping runs (Tootell et al., 1995). Two vertically or horizontally oriented wedges (15° width) composed of a flickering (0.125 Hz) color checkerboard pattern were presented for 16 s. Participants had no task to perform other than fixating at the center of the screen.

MRI data processing

Preprocessing: Functional scans were preprocessed using a standard preprocessing pipeline in SPM8. Preprocessing included slice timing correction; spatial realignment; estimation of coregistration parameters of the mean and all images to an anatomical image; and segmentation of the anatomical image, which, together with the coregistration parameters, was subsequently used for normalization to the MNI space, followed by smoothing with a 5.5-mm full-width half-maximum Gaussian kernel. An example of the entire batch processing script is available at https://bitbucket.org/qbilius/twolines.

Statistical model specification: To analyze experimental runs, we used t values, which were computed in SPM by contrasting parameter estimates for each condition against the fixation condition (per participant).

In the localizer and meridian-mapping runs, beta values were estimated with three independent variables for the localizer and two independent variables for meridian mapping.

Definition of regions of interest: ROIs were defined in Caret 5.65 (Van Essen et al., 2001) on a flattened image of the brain separately for each participant (Figure 3). First, the borders between three regions—V1 and V2, V2 and V3, and V3 and higher regions—were defined by observing where activations for the horizontal wedge were different from activations for the vertical wedge in the meridian-mapping runs. Using this border information, ROIs were selected based on the localizer runs. To identify ROIs in regions V1, V2, and V3, we identified areas in which activations for all stimuli were greater than activations during fixation blocks. For the shape-selective LO and pFs cortex, we identified brain regions in which activations for intact objects were greater than activations for scrambled objects (Grill-Spector et al., 1998). LO was defined as a lateral shape-selective region, and the pFs cortex was chosen on the ventral surface.

Degree of regularity computations

Based on the stimulus hierarchy, we computed the average neural response across each degree of regularity (per participant). Next, for each participant, we computed the slope of the fit of linear regression and tested whether the slope was significantly different from zero using a two-tailed one-sample t test.

Simulations

Gabor-Jet model: We employed a simple Gabor-Jet model (Lades et al., 1993; Fiser, Biederman, & Cooper, 1996) in order to compute the physical similarity of our stimuli and estimate to what extent various regions in the brain reflect it in fMRI signals. In this model, 100 locations from an image (on a 10×10 square grid) are convolved with Gabor filters of eight orientations (in steps of 22.5°) and five spatial frequencies, resulting in a vector with 4,000 elements. As this computation is done in the frequency domain, only the resulting magnitude (not phase) is used in subsequent computations.

Stimulus generation for modeling: Model responses were computed using the actual stimuli displays as shown to the participants during the experiments but scaled to 256×256 pixel size. Moreover, because stimuli were moving during the experiment, we used only a single (first) frame for each condition.

Comparison to norm-based encoding: We wanted to compare whether our findings could be explained by norm-based encoding (Leopold et al., 2006; Panis, Wagemans, de Beeck, 2011). To that end, we generated 40 images per condition, computed the average response of Gabor-Jet model outputs to these images, and calculated a dissimilarity between each pair of images f and g (Panis et al., 2011):

$$dissimilarity(f,g) = \sqrt{\frac{\sum_i (f_i - g_i)^2}{n}},$$

where n is vector length (number of pixels in each image for the pixel-wise model or the 4,000 components in the Gabor-Jet model), resulting in values between 0 and 256. Next, these similarities were averaged per condition, and the resulting values were correlated to the fMRI responses that they elicited. The idea behind this dissimilarity index is that the "norm" or most average stimulus would have the lowest dissimilarity averaged across all pairwise comparisons with other images.

We verified the validity of this approach by generating 12 L-junctions with an angle ranging from 180°·1/26 to 180°·12/26 in steps of 180°·1/26. As expected, this analysis showed that the norm stimuli (i.e., stimuli with the smallest dissimilarity value) are stimuli 6 (angle 180°·6/26) and 7 (angle 180°·7/26). Their dissimilarity was 0.21, compared to a dissimilarity of 0.34 for stimuli 1 and 12.

Results

In this experiment, we sought to investigate whether and how stimulus regularity is reflected in the visual cortex. In particular, if degree of regularity played a role in encoding stimuli, we should observe an increase or a decrease in response strength with an increase in the regularity measure. To test this hypothesis, we computed an average fMRI signal intensity (t values) in five common ROIs along the ventral visual pathway (Figure 3): early visual areas V1, V2, and V3, and higher-level shape-selective LO and pFs. Figure 4 summarizes our basic finding: An increase in stimulus regularity appears to correlate with a decrease in fMRI signal strength in LO.

We quantified this effect by first estimating a slope of this decrease using a linear regression (per participant) and then testing whether these slopes were consistently different from zero (Figure 4, right). This analysis revealed a robust effect of regularity in LO, two-tailed one-sample t test: $t(7) = 2.76$, $p = 0.028$, but not in other ROIs (ts < 1.86, ps > 0.10). In pFs, there is only a very small response overall, suggesting that we did not have a reliable signal in this region, which could be due to several causes (including small region size, lack of functional involvement with these simple stimuli). When the estimated slope in LO was compared against the slopes found in early visual regions V1, V2, and V3 (pooling across the three ROIs), no significant difference was found, two-tailed paired-samples t test: $t(7) = 0.23$, $p = 0.82$.

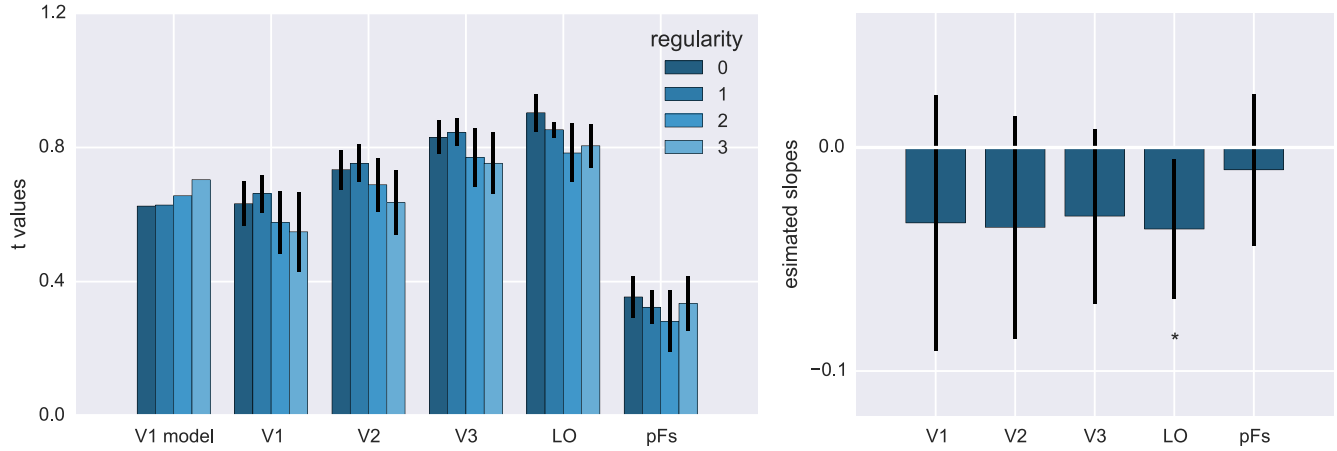

Figure 4. (Left) fMRI response dependency on the degree of stimulus regularity in each ROI and a V1 model output for comparison. Note a decrease in fMRI response to more regular configurations (degrees 2, 3). Error bars represent within-subject confidence intervals (Loftus & Masson, 1994; Cousineau, 2005; Morey, 2008). (Right) Slope of decrease of the fMRI response with an increase in stimulus regularity. Only LO shows a reliable dependency between the fMRI response and regularity ($p = 0.028$). Error bars represent 95% confidence intervals across participants.

Comparison to other definitions of regularity

We also tested if other possible definitions of regularity would yield a similar pattern of results. The regularity index used in our previous analysis is loosely based on the Minimal Model Theory (Feldman, 1997), which makes sense in the context of our stimulus set (Figure 1), and it was also the index that we used in our (chronologically) first analyses. However, several colleagues suggested that more formal definitions of regularity might make slightly different predictions (P. van der Helm, personal communication, March 8, 2013; J. Feldman, personal communication, March 19, 2013). In particular, stimulus ordering in Figure 1 is based on the Minimal Model Theory (Feldman, 1992, 1997) but computed for each of the three junction types separately (see Feldman, 2009, for discussion on choosing categories). We compared this definition to the regularity measures based on the strict version of Minimal Model Theory (i.e., no division into categories; Feldman, 1997) and another prominent theory of encoding, namely, the Structural Information Theory (SIT; Leeuwenberg & van der Helm, 2012; see Appendix for details). Neither of these more theoretical approaches could capture the observed decrease in fMRI signal (Minimal Model: ts < 1.4, ps > 0.21; SIT: ts < 0.74, ps > 0.48), possibly due to a pronounced categorization of stimuli into three junction groups (see "Junction index" in Methods).

Comparison to V1-like model outputs

To understand better the differences in representations in the defined ROIs, we employed a simple model of V1 (Lades et al., 1993; see Methods for details) as a means to quantify physical differences in stimuli. For each stimulus display, we computed a mean model response and correlated it with the mean fMRI responses in each ROI. Surprisingly, we found that this simple V1 model explained at least 44% of variance in the early visual areas (Pearson rs < -0.66, ps < 0.009). However, there was no correlation the between model's responses and the fMRI signal in the LO (LO: Pearson $r = -0.20$, $p = 0.27$; pFs: $r = 0.073$, $p = 0.41$). These findings indicate that the observed dependence on stimulus regularity emerges only in higher visual areas and is not driven by physical stimuli properties. In fact, if anything, model responses appear to show an opposite pattern of results: an increase in response to more regular stimuli (see Figure 4, left).

Is the effect different from norm-based encoding?

Finally, we investigated if the observed dependency on stimulus regularity could be a mere consequence of norm-based encoding. Norm-based encoding postulates that stimuli elicit the smallest responses when they are (physically) closest to the mean of the stimulus set (Leopold et al., 2006). Furthermore, this norm has been shown to be not some absolute "prototype" stimulus but rather to depend on the particular set that a participant was observing in an experiment, an effect that can emerge quickly over the course of an experiment (Kayaert, Op de Beeck, & Wagemans, 2011; Panis et al., 2011; Van Rensbergen & Op de Beeck, 2014). In order to quantify the norm in our stimulus set, we computed physical dissimilarities between all stimulus pairs using the same model of V1. If the observed effect is due to norm-based encoding, the "average" stimulus would be the least dissimilar from

others and would elicit the smallest response. We should therefore observe a robust positive correlation between the two measures. However, we did not observe any reliable relationship between the two measures in any ROI (absolute Pearson rs < 0.40, ps > 0.1), indicating that a different process than norm-based encoding was taking place.

Taken together, these results support the idea that encoding of simple visual stimuli composed of two lines is dependent upon the amount of regularity in their structure.

Experiment 2

In Experiment 1, we found that the fMRI signal was informative about stimulus regularity. However, the observed effect was small and based on a small number of participants. In Experiment 2, we wished to replicate the observed effect with a more powerful study (more imaging runs per participant) to investigate potential differences between early and higher visual areas. Moreover, we wanted to gain a deeper insight into the potential regularity encoding strategies: Is regularity only reflected in the overall fMRI response, or is it also encoded in the finer scale changes in the fMRI pattern of response? For example, observe that in our stimulus set regularity is dependent on right angles and midpoint intersections. It is possible that the visual cortex selectively optimizes processing of these features, leading to both a decrease in the overall fMRI response and changes in the pattern of responses. We could not address this question with the stimulus set in Experiment 1 because stimuli were not matched for their physical differences (V1 simulation results not shown). Some stimuli appeared to be easier to distinguish than other stimuli, making it difficult to know whether differences in decoding performance were due to genuine sensitivity to stimulus regularity or merely reflected differences in the physical stimulus similarity.

We therefore conducted a second experiment in which stimuli were matched in their physical similarity but had an unequal amount of regularity (Figure 5). For this task, we constructed a stimulus set based solely on the X-junction stimuli in Experiment 1 in order to have as much homogeneity in stimuli as possible. First, a "base" stimulus (e.g., a right-angle X-junction) was taken from Experiment 1. Then two more stimuli were created, one with an additional degree of regularity (e.g., a cross), and the other had the same regularity (thus a right-angle X-junction as well) but with a relevant property changed in the opposite direction (in this case, the position of intersection between the two lines was shifted to the left). Based on a similar manipulation used in the context of the generalized cones as well as in several psychophysical and developmental studies (Biederman, 1987; Vogels, Biederman, Bar, & Lorincz, 2001; Kayaert, Biederman, & Vogels, 2005; Ons & Wagemans, 2011), we call these changes "nonaccidental" and "metric."

Using this stimulus set, we performed Experiment 2 with a similar fMRI paradigm as in Experiment 1. Experiment 2 replicated our basic finding in Experiment 1, showing a robust sensitivity to stimulus regularity in LO. However, even with this more stringent design, we failed to observe reliable differences between nonaccidental and metric changes in the multivariate fMRI analysis. Our results indicate that stimulus regularity is reflected in a global decrease of fMRI response.

Methods

We used a very similar procedure to Experiment 1. Below only the relevant differences are described.

Participants

Eight affiliates of KU Leuven (ages 21–31, four male, four female) participated in the behavioral experiment (four of them participated in Experiment 1, which was conducted about half a year prior to Experiment 2). The experiment was approved by the committee for medical ethics at KU Leuven.

Stimuli

The stimulus set consisted of 13 two-line configurations, spanning 4° of regularity (Figure 5). In this experiment, we wanted to directly compare physically matched stimuli, so seven metric/base/nonaccidental triplets were defined using these stimuli in which metric and nonaccidental stimuli differed from the base stimulus to the same extent but in the opposite directions. Consider, for example, a generic X-junction in which the two lines intersect at a 70° angle. Its metric variant (also a generic X-junction) has a 20° change in angle, resulting in an intersection at a 50° angle. Its nonaccidental variant (a right-angle X-junction) also has a 20° change in angle, but in another direction, resulting in the intersection at a right angle and thus an increase in its regularity (a right-angle X-junction is a more regular, or "special," configuration than just a generic X-junction).

As compared to Experiment 1, stimuli were made wider and thinner (3° length and 0.1° line width) in order to enhance finer scale discrimination of stimulus properties.

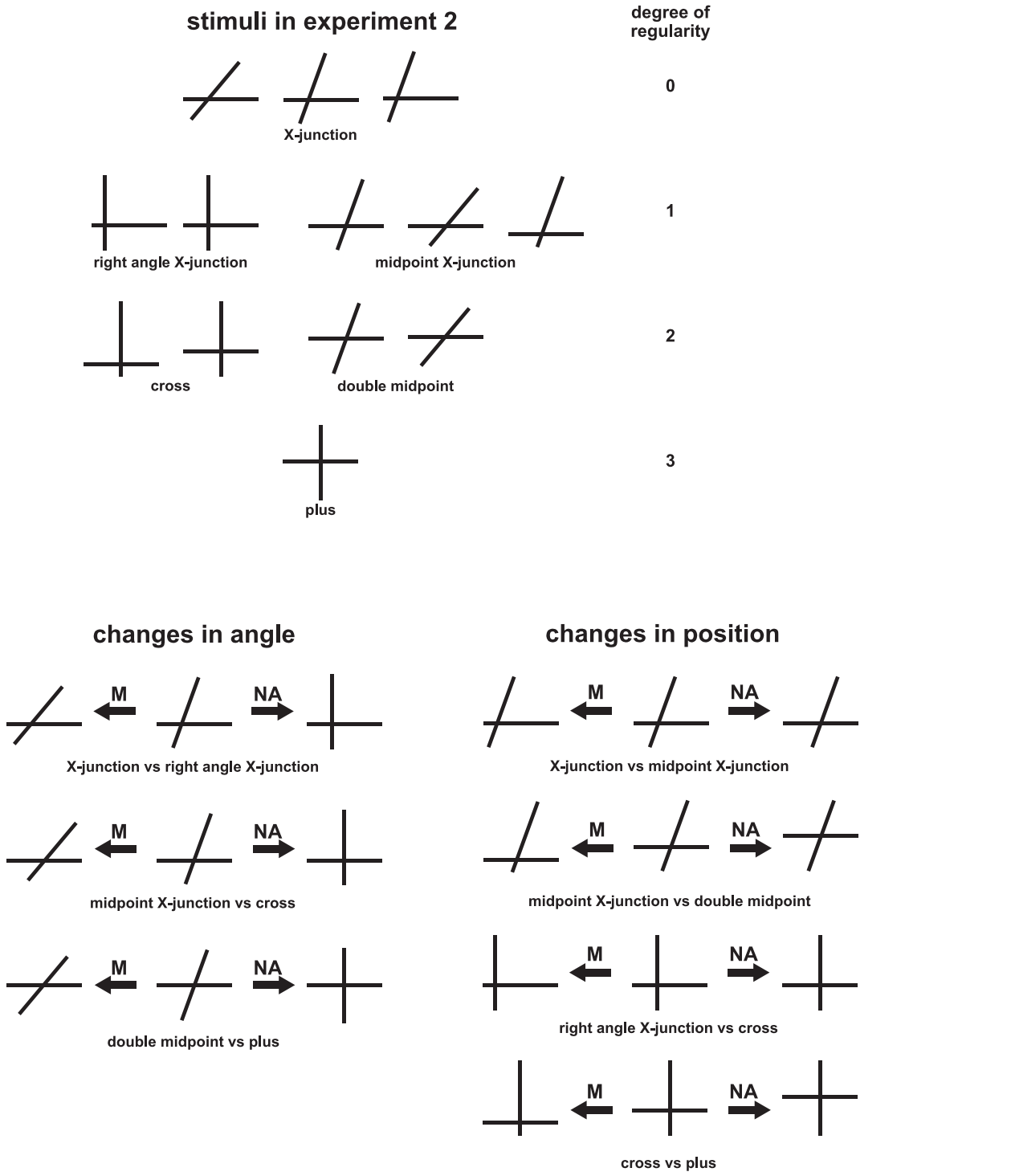

Figure 5. (Top) Stimuli in Experiment 2 ordered in terms of their regularity. (Bottom) Metric/base/nonaccidental X-junction triplets that can be formed using these stimuli. For changes in angle, the base stimulus has a 70° angle with its metric and nonaccidental variants at 50° and 90°, respectively. For changes in position, the base stimulus has an intersection at one third of the stimulus length with its metric and nonaccidental variants at one sixth and one half, respectively.

fMRI experiment and analysis details

The fMRI experiment consisted of two scan sessions, 2 h and 1.5 h long, during which participants completed between 28 and 32 runs of the main task (248 s each) and two localizer runs (if not available from Experiment 1; 336 s each) in total. For all participants, meridian-mapping and a high-resolution anatomical scan were used from previous studies. Otherwise,

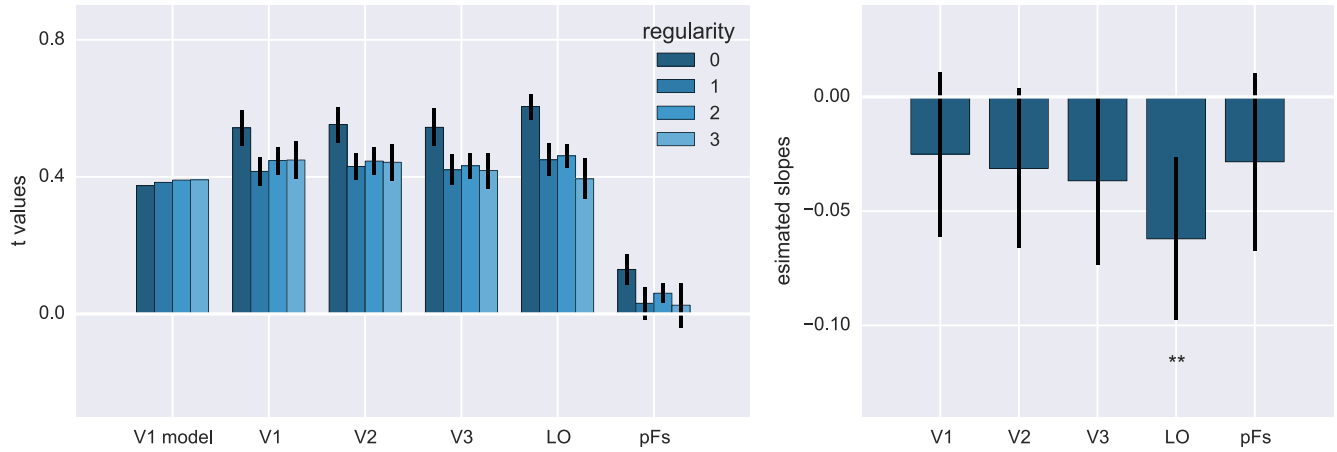

Figure 6. (Left) fMRI response dependency on the degree of stimulus regularity in each ROI and a V1 model output for comparison. Note a decrease in fMRI response to more regular configurations. Error bars represent within-subject confidence intervals (Loftus & Masson, 1994; Cousineau, 2005; Morey, 2008). (Right) Slope of decrease of the fMRI response with an increase in stimulus regularity. Only LO shows a reliable dependency between the fMRI response and regularity ($p = 0.004$). Error bars represent 95% confidence intervals across participants.

experimental and analysis procedure was identical to Experiment 1 with the addition of a multivoxel pattern analysis (MVPA) as detailed next.

MVPA analysis

fMRI data was processed using the PyMVPA2 package (Hanke et al., 2009). First, we normalized data by subtracting the mean and dividing by the standard deviation across voxels in each run for each condition separately (Misaki, Kim, Bandettini, & Kriegeskorte, 2010). For each pair of stimuli, a linear v support vector machine (SVM; from the LIBSVM package by Chang & Lin, 2011) was trained on all but eight runs in a pairwise classification task (i.e., for all pairwise combinations of stimuli) and then cross-validated on the average of the remaining eight runs. This procedure was repeated 100 times, each time using a random sample of cross-validation runs. Performance is reported as the proportion of correct identification of the test data labels.

Results

First, we confirmed that we could replicate the basic finding in Experiment 1, namely, the decrease in fMRI response in LO with an increase in stimulus regularity (Figure 6). We found that despite limiting the stimulus set to a single junction type, and thus vastly increasing

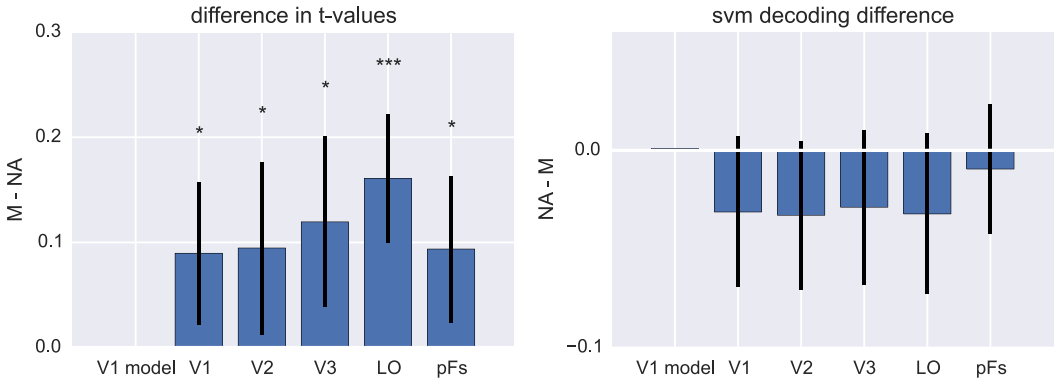

Figure 7. (Left) Differences in fMRI signal between metric and nonaccidental stimuli for stimuli triplets in Figure 5 (t values). Metric (M) stimuli (i.e., less regular) elicited stronger responses than nonaccidental (NA) stimuli in all ROIs, most robustly in LO. (Right) Differences in SVM decoding for stimuli triplets in Figure 5. Decoding of a metric versus base stimulus did not differ significantly from decoding a nonaccidental versus base stimulus with a trend of a higher similarity between the base and the nonaccidental variant, opposite to our prediction. Note that in both cases there was no difference based solely on physical stimulus properties (V1 model). Error bars represent 95% confidence intervals across participants.

homogeneity, the effect in LO was, in fact, even more pronounced, two-tailed one-sample t test: $t(7) = 4.13$, $p = 0.004$, consistent with the fact that the data was obtained from roughly 50% more imaging runs. However, in other ROIs (including pFs), the effect was not statistically significant ($ts < 1.86$, $ps > 0.10$). In fact, we found a reliable difference between the estimated slopes in LO and the early visual cortex, V1, V2, and V3 pooled together: two-tailed paired-samples t test: $t(7) = 2.93$, $p = 0.022$, suggesting potential differences in regularity encoding across the visual hierarchy.

Another way to look at regularity effects in the visual cortex is to compare responses to nonaccidental and metric stimuli in each triplet from Figure 5. By construction, nonaccidental stimuli are always more regular in a particular triplet than the metric ones. In accordance with this prediction, we found lower, on average, responses to nonaccidental stimuli than to metric stimuli (Figure 7, left), LO: $t(7) = 6.21$, $p < 0.001$, other ROIs: $ts > 2.73$, $ps < 0.029$.

Comparison to V1-like model outputs

We also computed responses of the V1 model to this stimulus set and compared them to the fMRI signal. Unlike in Experiment 1, we did not find a relationship between model responses and fMRI signal (absolute Pearson $rs < 0.10$, $ps > 0.37$), consistent with our choice to use a more homogenous set of stimuli (i.e., X-junctions) in this experiment. In particular, in Experiment 1 but not Experiment 2, there were vast differences between stimuli in terms of their junction type (see "Junction index" in Methods), potentially driving the robust correlation between model response and fMRI.

Moreover, in the norm-based encoding analysis, we also did not observe a reliable dependence between stimulus similarity and fMRI signal (Pearson $rs < 0.32$, $ps > 0.14$), further establishing regularity encoding as a separate process from norm-based encoding.

Support vector machine analysis

Next, we asked if differences in degree of regularity were reflected in the fMRI patterns of response. In particular, using a linear SVM, we computed the average decoding accuracy between each possible pair of stimuli (in each ROI). This accuracy reflects the amount of dissimilarity in stimuli: The greater the accuracy, the more distinctly the two stimuli are represented in that ROI. We compared dissimilarity for stimuli with the same degree of regularity (metric changes) to the stimuli with a difference in one degree of regularity (nonaccidental changes). We predicted that if regularity was reflected in the fMRI pattern of response, the computed dissimilarities should be greater for nonaccidental changes (in which there is a difference in degree of regularity) than for metric changes (in which both stimuli have the same amount of regularity). Note that despite these perceptual differences in the stimuli, they were well matched in terms of their physical similarity as shown by the V1 model simulation (Figure 7, right). Also note that fMRI response patterns were normalized to zero mean and a standard deviation of one (see Methods) so that only differences in response patterns but not in overall response magnitude or variance could be picked up by the classifier.

Contrary to our prediction, there was no consistent advantage in decoding nonaccidental stimuli pairs. If anything, there was a trend toward metric stimuli being more dissimilar than nonaccidental (two-tailed one-sample t test: $ts < 2.1$, $ps > 0.077$). Note that overall decoding was highly above chance (50%) for all stimuli—81% in early areas, $ts > 7.87$, $ps < 0.001$; 61% in LO, $t(7) = 9.18$, $p < 0.001$—as well as for the selected metric/nonaccidental comparisons—70% in early areas, $ts > 5.49$, $ps < 0.001$; 55% in LO, $t(7) = 4.56$, $p = 0.003$—suggesting that lack of difference was not caused by lack of power. We therefore conclude that sensitivity to the perceptual regularity is reflected in the overall signal intensity and not in the pattern of responses.

Discussion

Relationship between configural regularity and signal changes

In this study, we sought evidence that the visual system utilizes perceptual regularities in encoding stimuli. In two fMRI experiments, we observed a reliable dependency between the amount of regularity and fMRI signal intensity. The effect was most prominent in the higher-level shape-selective area LO where more regular configurations elicited smaller fMRI responses. In contrast, early areas of visual cortex appeared to reflect physical stimulus properties, significantly differing from representations in LO in Experiment 2. Interestingly, this result is consistent with behavioral, fMRI, and neurophysiological studies by Biederman and his collaborators (Biederman, 1987; Kayaert et al., 2005; Amir, Biederman, & Hayworth, 2011; Kim & Biederman, 2012) in which LO (in humans) or IT (in monkeys) have been reportedly found to be sensitive to nonaccidental changes (similar to our Experiment 2). In contrast to these studies, in which a full 3-D shape or at least a silhouette was used, we chose our stimuli to be simple to maximize chances

of observing any effect at lower visual areas. The fact that we failed to observe a dependency in these earlier regions suggests that regularity is more likely to be a higher-level computation even with simple pairs of line segments. However, given that all ROIs reflected dependency of configural regularity to some extent, differences between regularity encoding in lower and higher visual areas remains open for further investigations.

Configural regularity in SVM analyses

We further investigated the finer scale of the observed effect by comparing physically, but not perceptually, equidistant stimuli pairs. Although decoding of each stimulus type was highly above chance, indicating the reliability of the acquired data set, we could not find reliable finer-scale differences between nonaccidental and metric stimuli pairs. Note that following a standard SVM analysis practice (Misaki et al., 2010), response patterns were normalized to avoid classification based on differences in the overall magnitude or variance of responses(see Methods for details). Taken together, these results indicate that regularity computation is manifested not in finer-scale changes in the pattern of response but rather in the global modulation of an overall neural activity, most robustly in area LO.

When is regularity computed in the brain?

The observed reduction might reflect an increase in efficiency in coding stimuli in the system. In such an encoding scheme, the most regular shapes could be processed and stored using the smallest number of features or parameters, thus decreasing the amount of computation and the related neural activity. However, in this study, we used a very simple stimulus set in which only two parameters (angle and intersection position) controlled regularity. In contrast, natural scenes are much more complex, and a straightforward attempt to estimate stimulus regularity directly from the input is unlikely to succeed. Instead, we speculate that the computation of regularity is bound to higher visual areas such that it would only be computed after the shape is properly segmented from the background clutter, drastically reducing the complexity involved in such computation (Li, Cox, Zoccolan, & DiCarlo, 2009; MacEvoy & Epstein, 2009). For example, in these areas, representations might already encode the structure of an object in terms of boundary fragments (Kourtzi & Connor, 2011) or geons (Biederman, 1987). For such representations, encoding regularity increases the efficiency of the representation, and computing it is simple (Hummel & Biederman, 1992; Feldman, 1997). However, given the observed tendencies even in the lower visual areas to reflect the degree of regularity, and the poor temporal resolution of fMRI, the precise role of lower and higher visual areas in regularity computation remains elusive.

Relationship to set size

An alternative approach to interpreting our results comes from noting that more regular stimuli, by definition, belong to a smaller class of possible configurations (Garner, 1974): two lines can form many different X-junctions but only a single plus. Thus, it is plausible that the visual cortex has more "junction detectors" tuned to frequent, more generic configurations but few tuned to such unlikely configurations as a plus. This idea is, however, at odds with evidence for specialized detectors in the higher visual cortex. For example, Hegdé and Van Essen (2007) reported a dramatic increase in the number of neurons tuned to pluses in monkey V4 as compared to V2. Moreover, the prevalence of such feature detectors is likely shaped by natural input statistics, but the distribution of generic configurations in the natural input statistics is not clear and might be interesting to explore using large data sets of urban environments, such as Google maps (Doersch, Singh, Gupta, Sivic, & Efros, 2012).

Effect of symmetry

In a similar manner, it is also possible that the observed effect is, in fact, due only to symmetry in stimuli configurations rather than a broader class of configural regularities. In particular, notice that in both experiments, stimuli with the highest degrees of regularity (two or three) are necessarily symmetric, and lower degrees of regularity mostly do not lead to symmetries in stimuli. We tested this possibility by collapsing our data according to symmetry but found a significant difference only in V1 in Experiment 1, two-tailed paired-samples t test: $t(7) = 3.11$, $p = 0.017$. Moreover, notice that in the particular set that we used, several stimuli in level 1 (e.g., some of right-angle X-junctions) are also symmetric (see red numbers in Figure 9 in the Appendix for a visualization). When analyzed by strictly adhering to this categorization, our data does not show reliable differences between symmetric and asymmetric stimuli. Furthermore, symmetry is explicitly encoded in SIT but the theory fails to account for our data (see Appendix). Of course, it is possible that participants perceived these stimuli as coming from a larger class of stimuli (e.g., all right-angle X-junctions) that usually do not have these

regularities. In this case, however, a larger set of stimuli with more variation in degrees of regularity would be necessary to conclusively determine whether sensitivity to regularity can be driven by regularities other than symmetry.

Other definitions of regularity

Finally, we found that the observed pattern of results could not be explained using alternative approaches to regularity in the strict interpretation of the Minimal Model Theory and SIT (see Appendix). Such discrepancy is not new. For example, Feldman (2007) found a match between his theory and behavioral results for some but not all conditions that he investigated. Given their purely mathematical basis, these theories might be limited in the extent that they can account for neural data although we could not rule out the possibility that regularity computations adhering to these theories might be implemented somewhere in the brain. Moreover, notice that while our results are not explained by the Minimal Model Theory in its strict sense, it is nonetheless quite compatible with it when stimulus ordering is computed within chosen categories as discussed by Feldman (2009). Finally, we used a very restricted set of stimuli with only a few parameters changing across stimuli, so it is possible that in a wider set defined by more parameters we would have observed a greater consistency with one or both of these theories. However, this study was not designed to compare these theories but rather to investigate whether they carry any relevance to the neural processing of visual information. Our results show that they do.

Keywords: regularity, encoding, grouping, perceptual organization, fMRI

Acknowledgments

This work was supported by a Methusalem Grant (METH/08/02) awarded to Johan Wagemans from the Flemish Government and the Inter-Universitaire-Attractie-Polen (IUAP) grant P7/11 awarded to Hans P. Op de Beeck. Jonas Kubilius is a research assistant of the Research Foundation – Flanders (FWO). We thank Ronald Peeters for technical assistance with the fMRI scanning, and Pascaline Vancraeyenest, Bart Michiels, and Stef Van Puyenbroeck for their help in producing cortical flat maps in Caret. We also thank Charlotte Sleurs for fruitful discussions, Peter van der Helm and Jacob Feldman for their assistance in computing stimulus regularity according to various measures, and Pieter Moors for help and discussions on statistical analyses. Statement of Open Science: For maximal transparency, this research was carried out using as many free and open source software tools as possible, including GNU/Linux, Python (PsychoPy, psychopy_ext, pandas, and their dependencies), R, JAGS, Mercurial (hg), LyX, SPM, and Caret. Full source code of the entire study is available at https://bitbucket.org/qbilius/twolines; all data sets, due to their size, are available upon request.

Commercial relationships: none.
Corresponding author: Hans P. Op de Beeck.
Email: Hans.OpdeBeeck@ppw.kuleuven.be.
Address: Laboratory of Biological Psychology, KU Leuven, Leuven, Belgium.

References

Amir, O., Biederman, I., & Hayworth, K. J. (2011). The neural basis for shape preferences. *Vision Research, 51*(20), 2198–2206, doi:10.1016/j.visres.2011.08.015.

Attneave, F. (1954). Some informational aspects of visual perception. *Psychological Review, 61*(3), 183–193, doi:10.1037/h0054663.

Attneave, F. (1959). *Applications of information theory to psychology: A summary of basic concepts, methods, and results (Vol. vii)*. Oxford, England: Henry Holt.

Barlow, H. B. (1961). Possible principles underlying the transformation of sensory messages. In W. Rosenblith (Ed.), *Sensory communication,* (pp. 217–234). Cambridge, MA: MIT Press.

Biederman, I. (1987). Recognition-by-components: A theory of human image understanding. *Psychological Review, 94*(2), 115–147, doi:10.1037/0033-295X.94.2.115.

Chang, C.-C., & Lin, C.-J. (2011). LIBSVM: A library for support vector machines. *ACM Transactions on Intelligent Systems and Technology*, *2*(3), *27,* 1–27.

Cousineau, D. (2005). Confidence intervals in within-subject designs: A simpler solution to Loftus and Masson's method. *Tutorials in Quantitative Methods for Psychology*, *1*(1), 42–45.

DiCarlo, J. J., & Cox, D. D. (2007). Untangling invariant object recognition. *Trends in Cognitive Sciences, 11*(8), 333–341, doi:10.1016/j.tics.2007.06.010.

Doersch, C., Singh, S., Gupta, A., Sivic, J., & Efros, A. A. (2012). What makes Paris look like Paris? *ACM Transactions on Graphics*, *31*(4), *101,* 1–101, doi:10.1145/2185520.2185597.

Doi, E., Gauthier, J. L., Field, G. D., Shlens, J., Sher, A., Greschner, M., ... Simoncelli, E. P. (2012).

Efficient coding of spatial information in the primate retina. *The Journal of Neuroscience, 32*(46), 16256–16264, doi:10.1523/JNEUROSCI.4036-12.2012.

Feldman, J. (1992). Constructing perceptual categories. In *Computer vision and pattern recognition, 1992. Proceedings CVPR '92, 1992 IEEE Computer Society Conference on* (pp. 244–250). Los Alamitos, CA: IEEE Computer Society Press. doi:10.1109/CVPR.1992.223268.

Feldman, J. (1997). Regularity-based perceptual grouping. *Computational Intelligence, 13*(4), 582–623, doi:10.1111/0824-7935.00052.

Feldman, J. (2003). Perceptual grouping by selection of a logically minimal model. *International Journal of Computer Vision, 55*(1), 5–25, doi:10.1023/A:1024454423670.

Feldman, J. (2007). Formation of visual "objects" in the early computation of spatial relations. *Perception & Psychophysics, 69*(5), 816–827, doi:10.3758/BF03193781.

Feldman, J. (2009). Bayes and the simplicity principle in perception. *Psychological Review, 116*(4), 875–887, doi:10.1037/a0017144.

Fiser, J., Biederman, I., & Cooper, E. E. (1996). To what extent can matching algorithms based on direct outputs of spatial filters account for human object recognition? *Spatial Vision, 10*(3), 237–271, doi:10.1163/156856896X00150.

Friston, K. (2009). The free-energy principle: A rough guide to the brain? *Trends in Cognitive Sciences, 13*(7), 293–301, doi:10.1016/j.tics.2009.04.005.

Garner, W. R. (1974). *The processing of information and structure (Vol. xi)*. Oxford, England: Lawrence Erlbaum.

Geisler, W. S., Perry, J. S., Super, B. J., & Gallogly, D. P. (2001). Edge co-occurrence in natural images predicts contour grouping performance. *Vision Research*, *41*(6), 711–724.

Grill-Spector, K., Kushnir, T., Hendler, T., Edelman, S., Itzchak, Y., & Malach, R. (1998). A sequence of object-processing stages revealed by fMRI in the human occipital lobe. *Human Brain Mapping, 6*(4), 316–328, doi:10.1002/(SICI)1097-0193(1998)6:4<316::AID-HBM9>3.0.CO;2-6.

Hanke, M., Halchenko, Y., Sederberg, P., Hanson, S., Haxby, J., & Pollmann, S. (2009). PyMVPA: A Python toolbox for multivariate pattern analysis of fMRI data. *Neuroinformatics, 7*(1), 37–53, doi:10.1007/s12021-008-9041-y.

Hegdé, J., & Van Essen, D. C. (2007). A comparative study of shape representation in macaque visual areas V2 and V4. *Cerebral Cortex, 17*(5), 1100–1116, doi:10.1093/cercor/bhl020.

Hummel, J. E., & Biederman, I. (1992). Dynamic binding in a neural network for shape recognition. *Psychological Review, 99*(3), 480–517, doi:10.1037/0033-295X.99.3.480.

Kayaert, G., Biederman, I., & Vogels, R. (2005). Representation of regular and irregular shapes in macaque inferotemporal cortex. *Cerebral Cortex, 15*(9), 1308–1321, doi:10.1093/cercor/bhi014.

Kayaert, G., Op de Beeck, H. P., & Wagemans, J. (2011). Dynamic prototypicality effects in visual search. *Journal of Experimental Psychology: General, 140*(3), 506–519, doi:10.1037/a0023494.

Kim, J. G., & Biederman, I. (2012). Greater sensitivity to nonaccidental than metric changes in the relations between simple shapes in the lateral occipital cortex. *NeuroImage, 63*(4), 1818–1826, doi:10.1016/j.neuroimage.2012.08.066.

Kourtzi, Z., & Connor, C. E. (2011). Neural representations for object perception: Structure, category, and adaptive coding. *Annual Review of Neuroscience, 34*(1), 45–67, doi:10.1146/annurev-neuro-060909-153218.

Kubilius, J. (2014). A framework for streamlining research workflow in neuroscience and psychology. *Frontiers in Neuroinformatics, 7, 52*, doi:10.3389/fninf.2013.00052.

Lades, M., Vorbruggen, J. C., Buhmann, J., Lange, J., von der Malsburg, C., Wurtz, R. P., & Konen, W. (1993). Distortion invariant object recognition in the dynamic link architecture. *IEEE Transactions on Computers, 42*(3), 300–311, doi:10.1109/12.210173.

Leeuwenberg, E., & van der Helm, P. A. (2012). *Structural information theory: The simplicity of visual form*. Cambridge University Press.

Leopold, D. A., Bondar, I. V., & Giese, M. A. (2006). Norm-based face encoding by single neurons in the monkey inferotemporal cortex. *Nature, 442*(7102), 572–575, doi:10.1038/nature04951.

Leopold, D. A., O'Toole, A. J., Vetter, T., & Blanz, V. (2001). Prototype-referenced shape encoding revealed by high-level aftereffects. *Nature Neuroscience, 4*(1), 89–94, doi:10.1038/82947.

Li, N., Cox, D. D., Zoccolan, D., & DiCarlo, J. J. (2009). What response properties do individual neurons need to underlie position and clutter "invariant" object recognition? *Journal of Neurophysiology, 102*(1), 360–376, doi:10.1152/jn.90745.2008.

Loftus, G. R., & Masson, M. E. J. (1994). Using confidence intervals in within-subject designs.

Psychonomic Bulletin & Review, 1(4), 476–490, doi: 10.3758/BF03210951.

MacEvoy, S. P., & Epstein, R. A. (2009). Decoding the representation of multiple simultaneous objects in human occipitotemporal cortex. *Current Biology, 19*(11), 943–947, doi:10.1016/j.cub.2009.04.020.

Misaki, M., Kim, Y., Bandettini, P. A., & Kriegeskorte, N. (2010). Comparison of multivariate classifiers and response normalizations for pattern-information fMRI. *NeuroImage, 53*(1), 103–118, doi:10.1016/j.neuroimage.2010.05.051.

Morey, R. D. (2008). Confidence intervals from normalized data: A correction to Cousineau (2005). *Tutorial in Quantitative Methods for Psychology*, *4*(2), 61–64.

Ons, B., & Wagemans, J. (2011). Development of differential sensitivity for shape changes resulting from linear and nonlinear planar transformations. *I-Perception, 2*(2), 121–136, doi:10.1068/i0407.

Op de Beeck, H., Wagemans, J., & Vogels, R. (2003). Asymmetries in stimulus comparisons by monkey and man. *Current Biology, 13*(20), 1803–1808, doi: 10.1016/j.cub.2003.09.036.

Panis, S., Wagemans, J., & de Beeck, H. P. O. (2011). Dynamic norm-based encoding for unfamiliar shapes in human visual cortex. *Journal of Cognitive Neuroscience, 23*(7), 1829–1843, doi:10.1162/jocn.2010.21559.

Peirce, J. W. (2007). PsychoPy—Psychophysics software in Python. *Journal of Neuroscience Methods, 162*(1–2), 8–13, doi:10.1016/j.jneumeth.2006.11.017.

Peirce, J. W. (2009). Generating stimuli for neuroscience using PsychoPy. *Frontiers in Neuroinformatics, 2, 10*,doi:10.3389/neuro.11.010.2008.

Rhodes, G., & Jeffery, L. (2006). Adaptive norm-based coding of facial identity. *Vision Research, 46*(18), 2977–2987, doi:10.1016/j.visres.2006.03.002.

Rock, I. (1983). *The logic of perception*. Cambridge, MA: MIT Press.

Sigman, M., Cecchi, G. A., Gilbert, C. D., & Magnasco, M. O. (2001). On a common circle: Natural scenes and Gestalt rules. *Proceedings of the National Academy of Sciences, USA, 98*(4), 1935–1940.

Simoncelli, E. P., & Olshausen, B. A. (2001). Natural image statistics and neural representation. *Annual Review of Neuroscience, 24*(1), 1193–1216, doi:10.1146/annurev.neuro.24.1.1193.

Tootell, R., Reppas, J., Kwong, K., Malach, R., Born, R., Brady, T., ... Belliveau, J. W. (1995). Functional analysis of human MT and related visual cortical areas using magnetic resonance imaging. *Journal of Neuroscience, 15*(4), 3215–3230.

van der Helm, P. A. (2014). *Simplicity in vision: A multidisciplinary account of perceptual organization*. Cambridge, UK: Cambridge University Press.

Van Essen, D. C., Drury, H. A., Dickson, J., Harwell, J., Hanlon, D., & Anderson, C. H. (2001). An integrated software suite for surface-based analyses of cerebral cortex. *Journal of the American Medical Informatics Association, 8*(5), 443–459, doi:10.1136/jamia.2001.0080443.

van Lier, R., van der Helm, P., & Leeuwenberg, E. (1994). Integrating global and local aspects of visual occlusion. *Perception, 23*(8), 883–903, doi:10.1068/p230883.

Van Rensbergen, B., & Op de Beeck, H. P. (2014). The role of temporal context in norm-based encoding of faces. *Psychonomic Bulletin & Review, 21*(1), 121–127, doi:10.3758/s13423-013-0478-0.

Vinje, W. E., & Gallant, J. L. (2000). Sparse coding and decorrelation in primary visual cortex during natural vision. *Science, 287*(5456), 1273–1276, doi: 10.1126/science.287.5456.1273.

Vogels, R., Biederman, I., Bar, M., & Lorincz, A. (2001). Inferior temporal neurons show greater sensitivity to nonaccidental than to metric shape differences. *Journal of Cognitive Neuroscience, 13*(4), 444–453, doi:10.1162/08989290152001871.

Wagemans, J., Elder, J. H., Kubovy, M., Palmer, S. E., Peterson, M. A., Singh, M., & von der Heydt, R. (2012). A century of Gestalt psychology in visual perception: I. Perceptual grouping and figure–ground organization. *Psychological Bulletin, 138*(6), 1172–1217, doi:10.1037/a0029333.

Wagemans, J., Feldman, J., Gepshtein, S., Kimchi, R., Pomerantz, J. R., van der Helm, P. A., & van Leeuwen, C. (2012). A century of Gestalt psychology in visual perception: II. Conceptual and theoretical foundations. *Psychological Bulletin, 138*(6), 1218–1252, doi:10.1037/a0029334.

Appendix: A comparison of different definitions of regularity

In this study, we used an intuitive notion of regularity, namely, that more constrained configurations are more regular. However, other authors have investigated the concept of regularity more extensively, building theoretical frameworks for regularity in visual perception. In this appendix, we consider and compare our results to two such prominent theories:

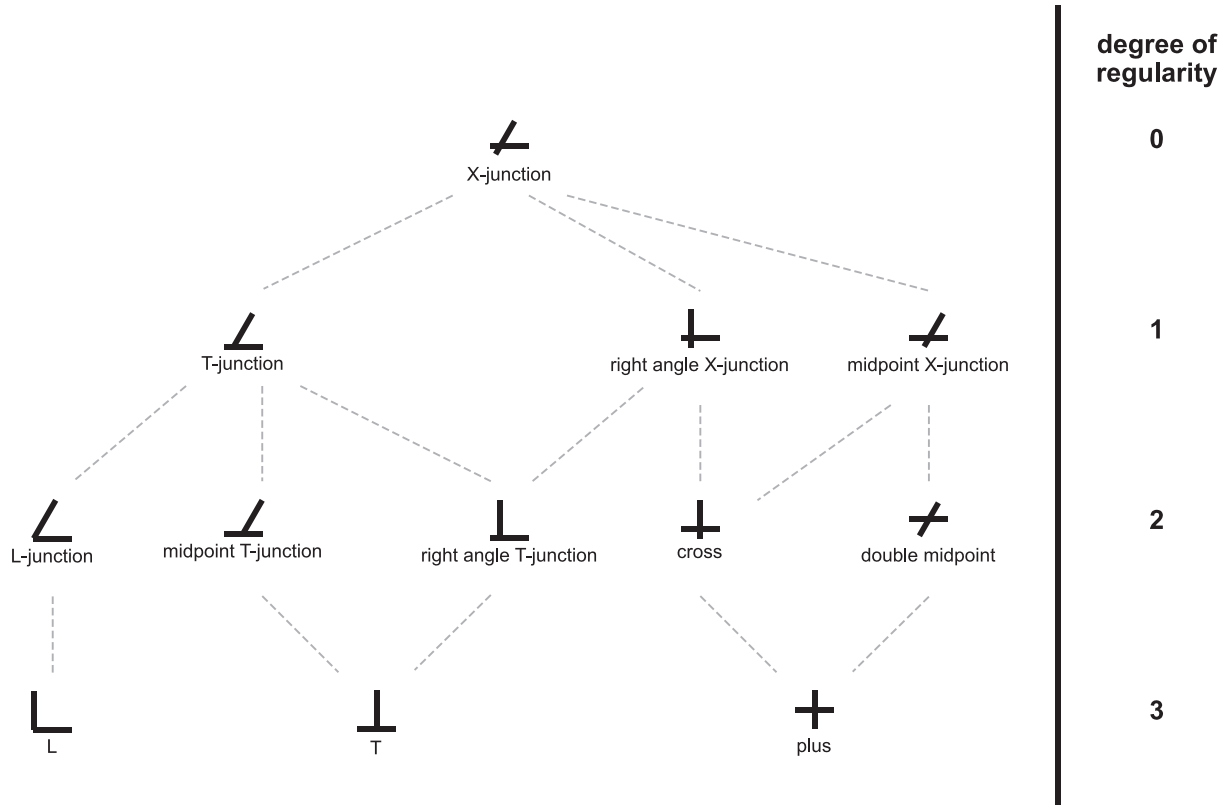

Figure 8. Stimulus set for Experiment 1 arranged according to stimulus regularity, or codimension, as it is known in the Minimal Model Theory (compare to figure 7 in Feldman, 1992).

Minimal Model Theory and Structural Information Theory.

Minimal Model Theory

Introduced by Feldman (1997), Minimal Model Theory defines regularity as "a class of configurations that an observer tends to utilize or recognize when it occurs." Although particular features that influence stimulus regularity are not stated by the theory, Feldman has proposed possible hierarchies of two-line configurations (Feldman, 1992) and investigated behavioral differences in their processing (Feldman, 2007). Our notion of regularity is based on this idea but with an additional division into subclasses (junction types) based on an intuition of what relevant classes could be (Feldman, 2009). In comparison, Figure 8 shows our stimulus set regularity for Experiment 1 according to the strict interpretation of the Minimal Model Theory.

Structural Information Theory

Regularity also plays in the Structural Information Theory (SIT; Van Lier et al., 1994; Leeuwenberg & van der Helm, 2012; van der Helm, 2014), which postulates that perceptually preferred interpretations are within the minimal information load and can be described by the shortest code or the least number of parameters (known as "the simplicity principle"). Unlike the Minimal Model Theory, which is oblivious to the kind of regularities used, SIT defines a set of operators, such as symmetry, that are used to describe stimuli. As such, SIT provides clear numerical predictions about stimulus complexity, which we here use as a measure of stimulus regularity. Figure 9 shows our stimulus set regularity for Experiment 1 and relevant computations according to the SIT.

Can these models explain the observed pattern of results?

We investigated whether these formulations of regularity could explain the observed pattern of results, namely, the decrease in fMRI signal with an increase in stimulus regularity. We performed the same degree of regularity analysis as explained in the main text but did not find any reliable relationship between fMRI signal and these regularity measures (Minimal Model: ts $<$ 1.4, ps $>$ 0.21; SIT: ts $<$ 0.74, ps $>$ 0.48).

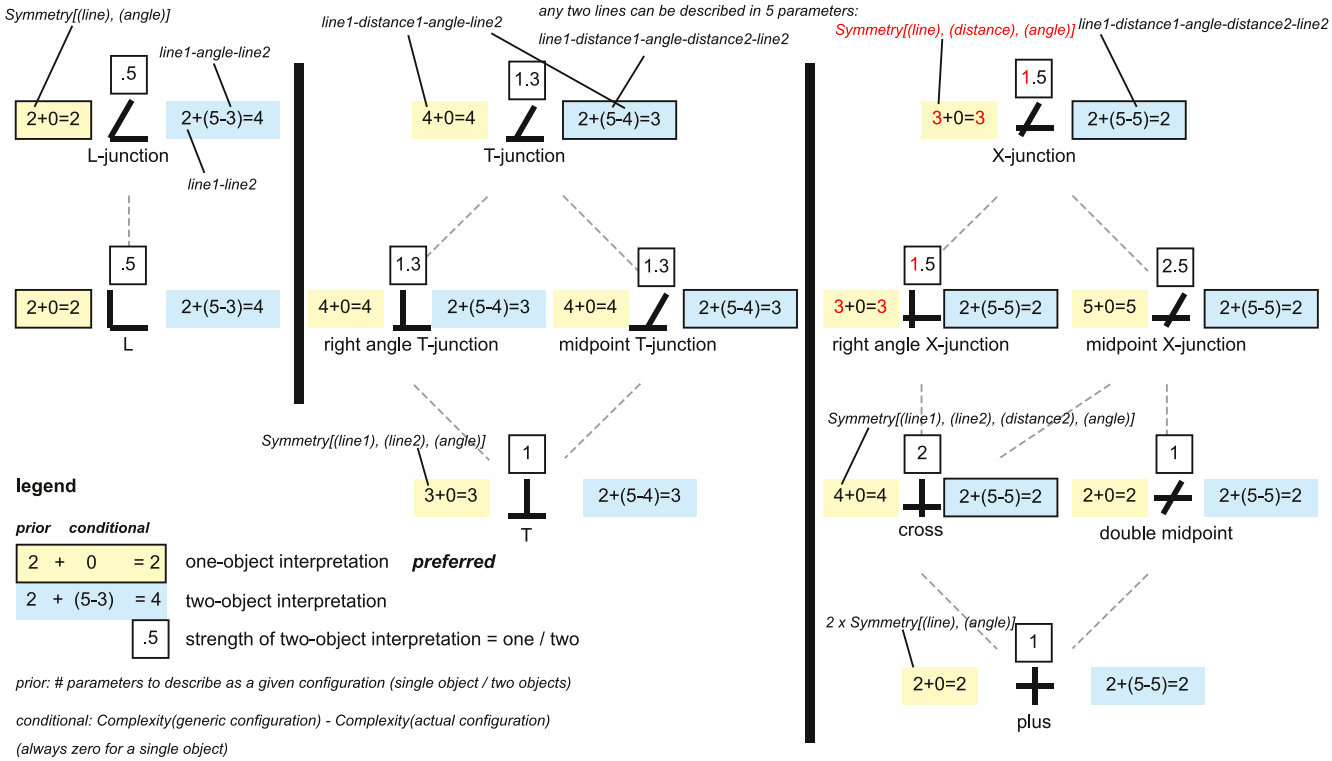

Figure 9. Stimulus set for Experiment 1 and structural complexity computations according to SIT. Yellow boxes indicate complexity for a one-object interpretation, and blue boxes show complexity for a two-object interpretation. White boxes indicate the strength of a two-object interpretation over a one-object interpretation, which we use as a final regularity measure to correlate with the fMRI signal.